Acoustic Determination of Thermophysical Properties and Critical Parameters for the Mixture (51 wt % R143a + 49 wt % R125) and Critical Line of xCO$_2$ + (1 − x)(51 wt % R143a + 49 wt % R125)

José M. S. S. Esperança, Pedro F. Pires,† Henrique J. R. Guedes, Nuno Ribeiro, Tânia Costa, and Ana Aguiar-Ricardo*

REQUIMTE/CQFB, Departamento de Química, Faculdade de Ciências e Tecnologia, Universidade Nova de Lisboa, 2829-516 Caparica, Portugal

The thermophysical properties and critical parameters for the alternative refrigerant (51 wt % of 1,1,1-trifluoroethane (R143a) + 49 wt % of pentafluoroethane (R125))—very close to the composition of R507 (50 wt % of each mixture component)—were investigated using two different acoustic techniques. The critical behavior of the system xCO$_2$ + (1 − x)(51 wt % R143a + 49 wt % R125) was also investigated. Experimental data of speed of sound in liquid (51 wt % R143a + 49 wt % R125) from T = (253 to 338) K and pressures up to 65 MPa were measured using a pulse-echo method. Derived thermodynamic properties were calculated, combining our experimental data with density and isobaric heat capacity values published by other authors. Measurements of the critical temperature T_c and pressure p_c on (51 wt % R143a + 49 wt % R125) and mixtures of xCO$_2$ + (1 − x)(51 wt % R143a + 49 wt % R125) were performed using another simple ultrasonic time-delay technique. The binary critical line was determined over the whole composition range showing that this system deviates only slightly from ideality since the critical line is a continuous line. The Peng−Robinson equation of state with conventional mixing and combining parameters was used to correlate the binary experimental data.

Introduction

As known, the hydrofluorocarbons (HFCs) are a new family of substances harmless toward the ozone layer since they do not contain chlorine. R507, an azeotropic binary mixture of HFC125 and HFC143a, is thought to be one of the most prospective substitutes to replace R502, an azeotropic mixture of HCFC22 and CFC115, almost exclusively used in low-temperature refrigeration.[1] It has physical and thermodynamic properties comparable to those of R502, is non-flammable, and the retrofit of existing R502 installations is possible.[2] As to environmental aspects, it has zero ozone depletion potential as compared to R502 (0.33) and a much lower halocarbon global warming potential (0.94) as compared to R502 (19.4). It has also been recognized[3] that the referred mixture is also a good replacement for HCFC22 and HCFC408A. The positive points to using our mixture or R507 instead the less expensive HCFC22 or HCFC408A are that our mixture or R507 is an HFC and that R408A is an HCFC. Because of the HCFC phase-out schedule, supplies of HCFC refrigerants could become limited while supplies of HFCs should always be available.

We have previously reported thermophysical properties and critical data on R404A and R410 as well as their mixtures with carbon dioxide.[4,5] In the present work, we extended our previous studies having measured the ultrasonic speed of propagation in liquid (51 wt % R143a + 49 wt % R125). The apparatus used has been tested and results reported for three other alternative refrigerants.[4−9] The experimental data were fitted and used together with density and isobaric heat capacity data from REFPROP[10] to calculate through an integration method[8,11−14] several thermodynamic properties, such as the isentropic and isothermal compressibilities (κ_S and κ_T), the isobaric thermal expansion coefficient (α_P), the thermal pressure coefficient (γ_V), the isenthalpic Joule−Thomson coefficient (μ_{JT}), and isobaric and isochoric heat capacities (C_p and C_V).

As stated before, recent works have shown that it seems likely that mixtures of new refrigerants rather than pure substances will replace the common CFCs. It is very important to have some accurate data concerning working fluids to develop industrial equipment (compressor, cooling equipment, etc). Nowadays, industry must be very careful about environment problems, limiting energy consumption, and costs. Vapor−liquid equilibrium data are required in order to evaluate the performance of refrigeration cycles. Moreover, apart from other important physicochemical properties, the knowledge of critical parameters is essential to design a simple process. Mixtures of partially fluorinated gases with CO$_2$ can be used as refrigerants or as modifiers to improve solubility in supercritical fluids. Therefore, knowledge of their phase behavior is crucial. In this work, critical properties of the system (51 wt % R143a + 49 wt % R125) and their mixtures with CO$_2$ were investigated. To that end, we have applied an acoustic simple technique that has proved to be a reliable method to explore the critical behavior of multicomponent systems as reported in previous works.[15−22] Measurements of the critical temperature T_c and pressure p_c of the xCO$_2$ + (1 − x)(51 wt % R143a + 49 wt % R125) mixtures were performed over the whole composition range. The Peng−Robinson equation of state, with conventional mixing and combining parameters, was used to correlate the experimental data.

* Corresponding author. Fax: +351 212948385. Tel: +351 212949648. E-mail: aar@dq.fct.unl.pt.
† Present address: CQM-Centro de Química da Madeira, Departamento de Química da Universidade da Madeira, Campus da Penteada, 9000-390 Funchal, Portugal.

10.1021/je060291c CCC: $33.50
Published on Web 09/28/2006

Table 1. Experimental Speed of Sound, u/m·s^{-1}, for Liquid Alternative Refrigerant Mixture (51 wt % R143a + 49 wt % R125) as a Function of Temperature T and Pressure p

T = 253.22 K		T = 258.15 K		T = 265.62 K		T = 273.14 K		T = 280.70 K		T = 288.18 K		T = 298.19 K		T = 308.19 K		T = 318.20 K	
p	u	p	u	p	u	p	u	p	u	p	u	p	u	p	u	p	u
MPa	m·s^{-1}	MPa	m·s^{-1}	MPa	m·s^{-1}	MPa	m·s^{-1}	MPa	m·s^{-1}	MPa	m·s^{-1}	MPa	m·s^{-1}	MPa	m·s^{-1}	MPa	m·s^{-1}
1.16	598.8	1.15	574.9	1.17	539.5	0.94	500.1	1.14	465.9	1.13	427.1	1.30	375.4	1.67	324.1	2.12	270.3
1.26	599.7	1.17	575.3	1.21	540.1	1.01	500.9	1.16	466.2	1.13	427.1	1.30	375.5	1.67	324.1	2.12	270.3
1.38	600.9	1.19	575.7	1.26	540.5	1.13	502.3	1.21	466.5	1.19	428.3	1.29	375.4	1.67	324.2	2.12	270.3
1.50	602.0	1.26	576.3	1.38	541.7	1.26	503.8	1.26	467.5	1.26	429.1	1.30	375.5	1.67	324.2	2.18	272.6
1.63	603.1	1.38	577.6	1.50	543.0	1.38	505.3	1.38	469.1	1.26	429.1	1.36	376.9	1.74	326.0	2.25	274.9
1.75	604.2	1.50	578.8	1.63	544.3	1.50	506.6	1.50	471.0	1.50	432.9	1.51	379.6	1.84	328.4	2.36	278.2
2.01	606.4	1.63	580.0	1.75	545.7	1.63	508.1	1.63	472.4	1.63	434.9	1.63	381.8	2.01	332.4	2.51	282.9
2.25	608.7	1.75	581.2	2.01	548.3	1.75	509.5	1.75	473.9	1.75	436.7	1.75	384.2	2.25	338.0	2.75	290.4
2.51	610.9	2.01	583.4	2.25	550.8	2.01	512.5	2.01	477.2	1.75	436.6	2.01	388.7	2.51	343.6	3.01	297.5
2.75	613.1	2.25	585.8	2.51	553.3	2.25	515.3	2.25	480.2	2.01	440.2	2.25	393.0	2.75	348.9	3.50	310.3
3.01	615.1	2.51	588.1	2.75	555.9	2.51	518.1	2.51	483.5	2.25	444.0	2.51	397.3	3.01	354.0	4.00	322.1
3.50	619.3	2.75	590.3	3.01	558.4	2.75	520.9	2.75	486.6	2.51	447.4	2.75	401.5	3.50	363.8	4.50	333.0
4.00	623.7	3.01	592.6	3.50	563.3	3.01	523.7	3.01	489.8	2.75	450.9	3.01	405.6	4.00	373.1	5.00	343.1
4.50	627.9	3.50	597.1	4.00	568.3	3.50	529.2	3.50	495.6	3.01	454.3	3.50	413.4	4.50	381.8	6.01	361.7
5.00	631.9	4.00	601.5	4.50	572.9	4.00	534.4	4.00	501.4	3.50	460.9	4.00	421.1	5.00	390.1	7.01	378.2
6.01	639.9	4.50	606.1	5.00	577.7	4.50	539.5	4.50	507.2	4.00	467.5	4.50	428.4	6.01	405.6	8.00	393.4
7.01	647.5	5.00	610.4	6.01	586.7	5.00	544.6	5.00	512.8	4.50	473.5	5.00	435.4	7.01	419.8	9.00	407.7
8.00	655.1	6.01	618.6	7.01	595.3	6.01	554.2	6.01	523.3	5.00	479.7	6.01	448.7	7.01	419.8	10.00	420.9
9.00	662.6	7.01	626.7	8.00	603.7	7.01	563.6	7.01	533.5	6.01	491.5	7.01	461.1	8.00	433.3	12.00	445.0
10.00	669.8	8.00	634.7	9.00	612.1	8.00	572.9	8.00	543.1	7.01	502.5	8.00	473.0	9.00	445.6	14.00	466.9
12.00	683.6	9.00	642.2	10.00	620.3	9.00	581.6	9.00	552.7	8.00	513.1	9.00	484.3	10.00	457.5	16.01	487.0
14.00	697.0	10.00	649.7	12.00	635.3	10.00	590.2	10.00	561.9	9.00	523.2	10.00	494.9	12.00	479.6	18.00	505.5
16.01	709.7	12.00	664.0	14.00	649.8	12.00	606.5	12.00	579.4	10.00	532.9	12.00	515.1	14.00	499.8	20.00	523.0
18.00	722.2	14.00	677.9	16.01	663.9	14.00	622.0	14.00	595.5	12.00	551.3	14.00	533.7	16.01	518.5	23.00	547.4
20.00	734.3	16.01	691.3	18.00	677.1	16.01	636.6	16.01	611.0	14.00	568.6	16.01	551.1	18.00	536.1	26.00	569.9
23.00	751.6	18.00	704.1	20.00	690.1	18.00	650.5	18.00	625.4	16.01	585.0	18.00	567.6	20.00	552.6	29.01	591.0
26.00	768.1	20.00	716.5	23.00	708.2	20.00	663.8	20.00	639.5	18.00	600.2	18.00	567.6	23.00	575.7	32.00	610.7
29.01	783.7	23.00	734.2	26.00	725.7	23.00	683.2	23.00	659.6	20.00	614.9	20.00	583.2	26.00	597.3	35.00	629.4
32.00	798.4	26.00	751.1	29.01	742.6	26.00	701.6	26.00	678.2	23.00	635.8	23.00	605.1	29.01	617.4	40.00	658.7
35.00	812.8	29.01	767.3	32.00	758.5	29.01	718.9	29.01	696.3	26.00	655.3	26.00	625.5	32.00	636.3	45.00	685.8
40.00	835.8	32.00	782.5	35.00	773.9	32.00	735.3	32.00	713.7	29.01	673.8	29.01	645.1	32.00	636.3	50.00	711.3
45.00	857.8	35.00	797.1	40.00	798.3	35.00	751.1	35.00	729.9	32.00	691.2	32.00	663.2	35.00	654.6	55.00	734.9
50.00	878.9	40.00	820.8	45.00	821.3	40.00	775.8	40.00	755.3	35.00	708.3	35.00	680.8	35.00	654.3	60.00	757.7
55.00	899.0	45.00	843.3	50.00	843.1	45.00	799.7	45.00	779.7	40.00	734.9	40.00	708.2	40.00	682.9	65.00	779.3
60.00	918.8	50.00	864.3	55.00	863.8	50.00	822.0	50.00	802.7	45.00	759.7	45.00	734.0	45.00	709.3		
65.00	937.2	55.00	884.5	60.00	883.7	55.00	843.4	55.00	824.2	50.00	783.2	50.00	758.0	50.00	734.0		
		60.00	904.1	65.00	902.8	60.00	863.4	60.00	845.1	55.00	805.1	55.00	780.7	55.00	757.3		
		65.00	923.1			65.00	882.8	65.00	864.9	60.00	826.3	55.00	780.9	55.00	757.1		
										65.00	846.7	60.00	802.3	60.00	779.5		
												60.00	802.4	60.00	779.5		
												65.00	823.1	65.00	800.7		
												65.00	823.1				

T = 328.17 K						T = 338.18 K					
p	u	p	u	p	u	p	u	p	u	p	u
MPa	m·s^{-1}	MPa	m·s^{-1}	MPa	m·s^{-1}	MPa	m·s^{-1}	MPa	m·s^{-1}	MPa	m·s^{-1}
2.66	211.8	6.01	316.6	23.00	520.4	3.38	154.6	7.01	293.8	26.00	519.0
2.66	211.9	7.01	336.3	26.00	543.8	3.44	160.1	8.00	314.4	29.01	541.7
2.66	211.8	8.00	353.7	29.01	565.9	3.50	165.9	9.00	333.0	32.00	563.0
2.66	211.8	8.00	354.0	32.00	586.4	3.66	178.1	10.00	349.3	35.00	583.0
2.66	211.8	8.00	353.9	35.00	605.5	3.83	189.0	12.00	378.7	40.00	613.8
2.75	216.9	9.00	370.0	35.00	605.8	4.00	199.1	14.00	404.3	45.00	642.4
2.88	223.4	10.00	384.7	40.00	635.7	4.25	211.1	16.01	427.4	50.00	669.0
3.01	229.4	12.00	411.3	45.00	663.5	4.50	221.8	18.00	448.3	55.00	693.9
3.50	249.7	14.00	435.1	50.00	689.5	5.00	240.3	20.00	467.8	60.00	717.2
4.00	266.3	16.01	456.6	55.00	714.1	6.01	269.8	23.00	494.6	65.00	739.8
4.50	280.9	18.00	476.5	60.00	737.1						
5.00	294.0	20.00	494.7	65.00	759.0						

Experimental Section

Materials. The mixture used in the experimental work was kindly supplied by Solvay Fluor und Derivate GmbH. According to the specifications of the manufacturer (Solvay), the mixture has a stated composition of 51 wt % of R143a and 49 wt % R125, being slightly different from the usual commercially accepted composition of R507 (50 wt % R143a + 50 wt % R125). The refrigerant mixture had a purity of 99.5 % and was used without further purification. CO_2 was supplied by Air Liquide and had a purity greater than 99.99 %. The mixtures were prepared in small stainless steel cylinders, and the compositions were determined by weighing.

Speed of Sound Measurements. The speed of sound of liquid (51 wt % R143a + 49 wt % R125) was measured with an apparatus designed for high pressures using a pulse-echo method at a frequency of 1 MHz as described in previous works.[4−9] The cell calibration was performed by measuring the speed of sound of pure CCl_4 at 10 MPa and 298.15 K and comparing the obtained value with data reported in the literature.[23,24] In order to cover the complete experimental temperature and

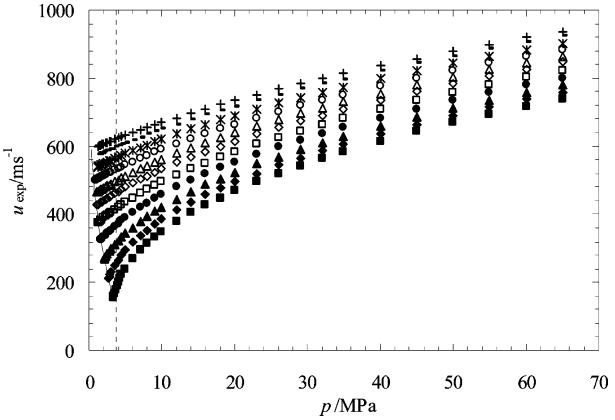

Figure 1. Experimental speed of sound, u, for liquid (51 wt % R143a + 49 wt % R125) as a function of pressure at the following: +, 253.22 K; −, 258.15 K; ∗, 265.62 K; ○, 273.14 K; △, 280.70 K; ◇, 288.18 K; □, 298.19 K; ●, 308.19 K; ▲, 318.20 K; ◆, 328.17 K; ■, 338.18 K; —, saturation line; - -, critical pressure.

pressure ranges, the calibration was expanded by the use of the thermal and pressure behavior of the pure copper spacers (purity better than 99.99 %). The calibration was tested with toluene and cyclohexane. Six data points at (298.15 and 320) K and pressures up to 40 MPa were measured for toluene, and 20 data points between (288.15 and 318.15) K and pressures up to 30 MPa were measured for cyclohexane. The literature data used in the toluene calibration[11] claim an accuracy of 0.1 m·s^{-1} or 0.01 %, and the data for cyclohexane[25] state an accuracy of 0.02 %. Taking into account all the error sources, the accuracy of the speed of sound measurements is estimated to be better than ± 0.3 m·s^{-1}. Several measurements were repeated at the same pressure and temperature conditions, allowing us to estimate a precision of ± 0.1 m·s^{-1}.

Measurements of Critical Data. The experimental apparatus for the critical data acquisition has already been described in detail[4,5,15,18] and was used unmodified in this study. A mixture with a desired composition was obtained by weighing and was pumped into the acoustic cell. The pressure was increased with the hand pump until only minute changes in the acoustic signal were observed, meaning that a liquid-like state with a low compressibility was present in the acoustic cell. The system was allowed to equilibrate for at least 30 min at the desired starting temperature. Experiments were carried out at constant temperature, and pressure was lowered until a maximum in time delay was observed. Temperature was then systematically varied and the procedure repeated. The temperature and pressure values corresponding to the absolute maximum of time delay in the ensemble of the isothermal curves (t_{delay}/μs vs p/MPa) were taken as the critical temperature and critical pressure.

Results

Speed of Sound of Liquid (51 wt % R143a + 49 wt % R125). The apparatus was used to take a total of 414 experimental speed of sound measurements of the alternative refrigerant mixture (51 wt % R143a + 49 wt % R125), at temperatures between (253.15 and 338.15) K and pressures up to 65 MPa. These data are shown in Table 1. The measurements were performed and organized within a total of 11 isotherms and are plotted in Figure 1. Fitting each one tested the consistency of the individual isotherms:

$$u/\mathrm{m\cdot s^{-1}} = \sum_{i=0}^{2} A_i[\ln(p/\mathrm{MPa} - B_i)]^i \qquad (1)$$

Table 2. Orthobaric Speed of Sound Data for Liquid (51 wt % R143a + 49 wt % R125)

T/K	p_σ/MPa	u_σ/m·s^{-1}	T/K	p_σ/MPa	u_σ/m·s^{-1}
253.22	0.32	590.9[a]	298.19	1.29	375.4
258.15	0.38	567.7[a]	308.19	1.66	324.2
265.62	0.49	532.0[a]	318.20	2.11	270.3
273.14	0.63	496.2[a]	328.17	2.64	211.8
280.70	0.79	461.1[a]	338.18	3.28	145.4[a]
288.18	0.98	424.7[a]			

[a] Extrapolated value.

Table 3. Coefficients of Equation 2 for the Orthobaric Speed of Sound, u_σ, of Liquid (51 wt % R143a + 49 wt % R125)

i	a_i
0	1.042297E+02
1	−2.553738E+03
2	−6.563941E+03
3	−1.638247E+04
4	−1.709840E+04

The standard deviations of the fits are smaller than 0.16 m·s^{-1} for isotherms in which the reduced temperature is lower than 0.95. For the isotherms at (328 and 338) K, which correspond to reduced temperatures of 0.95 and 0.98, the standard deviations of the fits are (0.27 and 0.52) m·s^{-1}, respectively. This increase in the standard deviation of the fits can be explained by the proximity of the critical temperature and, consequently, abrupt changes in the speed of sound measures when we are close to the critical point, as can be seen in Figure 1.

It was possible to measure the saturated liquid (orthobaric) speed of sound, u_σ, for the isotherms between (298 and 328) K. In the cases where the direct measurement was not possible, eq 1 was used to extrapolate the speed of sound at this temperature to the vapor pressure (REFPROP[10]). The orthobaric speed of sound data presented in Table 2 were fitted to

$$u_\sigma/\mathrm{m\cdot s^{-1}} = \sum_{i=0}^{4} a_i \cdot \left[\ln \frac{(T/\mathrm{K})}{(T_c/\mathrm{K})}\right]^i \qquad (2)$$

(critical data T_c = 344.04 K) with the coefficients of Table 3. The standard deviation of the fit was 0.46 m·s^{-1}.

Finally, the set of experimental data excluding the isotherm at 338 K was fitted to

$$u/\mathrm{m\cdot s^{-1}} = \frac{\sum_{i=0}^{2}\sum_{j=0}^{2} a_{ij}(p/\mathrm{MPa})^i(T/\mathrm{K})^j}{\sum_{k=0}^{2}\sum_{l=0}^{2} b_{kl}(p/\mathrm{MPa})^k(T/\mathrm{K})^l} \qquad (3)$$

with the coefficients shown in Table 4 and a standard deviation of 0.46 m·s^{-1}. The comparison between our fitted speed of sound data and the results obtained from REFPROP[10] are presented in Figure 2. The deviations are slightly high, but this can be related with the mixing parameters or with the functional form used in the commercial package.

As far as we are aware of, there is only one set of data for liquid R507 at orthobaric temperatures between T = (293 to 343) K.[26] Our data are higher than these by about 6.5 m·s^{-1} except for 338 K, where the deviation increases to 9.7 m·s^{-1}. These differences are higher than the estimated uncertainties of both experiments. However, REFPROP[10] data are also consistently higher than the ones from Fröba et al.[26] by about (6 to 9) m·s^{-1}. To the best of our knowledge, there are no other

Table 4. Coefficients of Equation 3 for the Speed of Sound of Liquid (51 wt % R143a + 49 wt % R125), Valid from T = (253 to 328) K and Pressures from Saturation Up to 65 MPa

a_{ij}	j		
i	0	1	2
0	1.6768423E+03	−9.3543620E+00	1.2910642E-02
1	−6.2711456E+01	4.8177950E-01	−8.4130084E-04
2	2.6431538E-01	−3.7446377E-03	1.0903584E-05
b_{kl}	l		
k	0	1	2
0	1	−3.1645171E-03	5.1019649E-07
1	−5.2210713E-02	3.1311440E-04	−3.3878384E-07
2	6.1850304E-04	−5.8826747E-06	1.3604166E-08

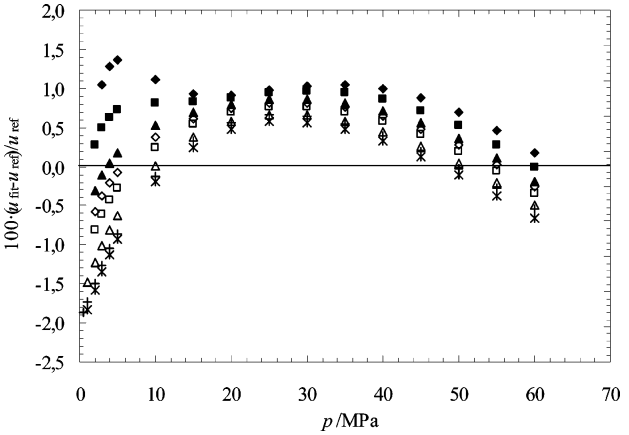

Figure 2. Percentage deviations $\{100\cdot(u_{fit} - u_{ref})/u_{ref}\}$ of the calculated speed of sound, u_{fit}, to REFPROP[10] data, u_{ref}, of (51 wt % R143a + 49 wt % R125): +, 260 K; ∗, 270 K; △, 280 K; □, 290 K; ◇, 295 K; ▲, 300 K; ■, 310 K; ◆, 320 K.

experimental speed of sound data to which the present work can be compared with.

Derived Thermodynamic Properties. The speed of sound, u, is directly related to the pressure derivative of the density, ρ, through eq 4, in which the subscript S denotes the condition of constant entropy:

$$\left(\frac{\partial\rho}{\partial p}\right)_S = \frac{1}{u^2} \tag{4}$$

This derivative is related to the isothermal pressure derivative and the isobaric temperature derivative of the density through eq 5, where C_p is the specific heat capacity at constant pressure:

$$\left(\frac{\partial\rho}{\partial p}\right)_S = \left(\frac{\partial\rho}{\partial p}\right)_T - \frac{T}{\rho^2 C_p}\left(\frac{\partial\rho}{\partial T}\right)_p^2 \tag{5}$$

Rearranging the last equation and combining it with eq 4 follows eq 6, which also incorporates the definition of the thermal expansion coefficient, α_p:

$$\left(\frac{\partial\rho}{\partial p}\right)_T = \frac{1}{u^2} + \frac{T}{C_p}\alpha_p^2 \tag{6}$$

$$\alpha_p = -\frac{1}{\rho}\left(\frac{\partial\rho}{\partial T}\right)_p \tag{7}$$

It can also be shown that the pressure partial derivative of the isobaric heat capacity can be calculated with

$$\left(\frac{\partial C_p}{\partial p}\right)_T = -\frac{T}{\rho}\left[\alpha_p^2 + \left(\frac{\partial\alpha_p}{\partial T}\right)_p\right] \tag{8}$$

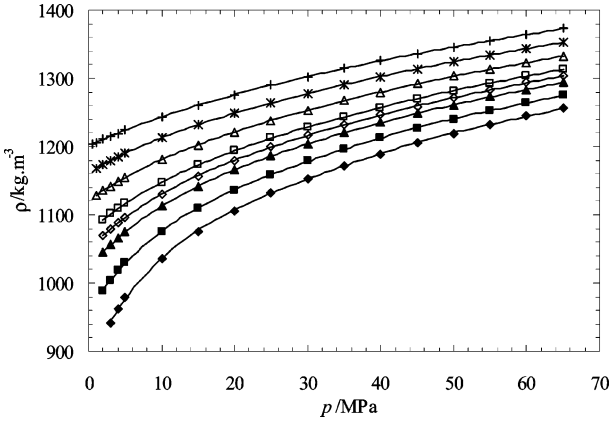

Figure 3. Density data of liquid (51 wt % R143a + 49 wt % R125), calculated through the integration procedure, as a function of pressure: +, 260 K; ∗, 270 K; △, 280 K; □, 290 K; ◇, 295 K; ▲, 300 K; ■, 310 K; ◆, 320 K.

Table 5. Coefficients Used To Fit the Literature Density, d_i, and Heat Capacity Data, c_j, with Equations 14 and 15, Respectively

i	d_i	c_j
0	−2.298838E+05	−6.811542E+06
1	5.020957E+03	1.730915E+05
2	−4.529419E+01	−1.882150E+03
3	2.175220E-01	1.135455E+01
4	−5.869462E-04	−4.104570E-02
5	8.439373E-07	8.891545E-05
6	−5.054158E-10	−1.068840E-07
7		5.500754E-11

This way, given an isobar of the density and of C_p, it is possible to integrate eqs 6 and 8 over the pressure, thus obtaining the (p, ρ, T) and (p, C_p, T) data points within the range of pressure and temperature of the experimental speed of sound data. The numerical integration procedure also allows, through the use of well established thermodynamic relationships, the calculation of other properties, such as the isentropic compressibility (κ_S), the isothermal compressibility (κ_T), the isochoric heat capacity (C_V), the thermal pressure coefficient (γ_V), and the isenthalpic Joule−Thomson coefficient (μ_{JT}).

In the present work, due to the scarcity of experimental density available and as to the best of our knowledge no isobaric heat capacity data exist in literature, the authors used data from the commercial available program REFPROP[10] at a pressure of 5 MPa and temperature from (250 to 330) K. These isobars were fitted to eqs 9 and 10 with the coefficients of Table 5:

$$\rho(T, 5\text{ MPa})/\text{kg}\cdot\text{m}^{-3} = \sum_{i=0}^{6} d_i (T/\text{K})^i \tag{9}$$

$$C_p(T, 5\text{MPa})/\text{J}\cdot\text{K}^{-1}\cdot\text{kg}^{-1} = \sum_{j=0}^{7} c_j (T/\text{K})^j \tag{10}$$

The integration procedure was implemented both on increasing pressure, up to 65 MPa, and on decreasing pressure, down to the saturation line.

The (p, ρ, T) data points obtained using the integration procedure are shown in Figure 3 and Table 6. In order to test the results, the whole set of calculated density data were fitted with an equation similar to eq 3, with a standard deviation of 0.008 %. Figure 4 shows the percentage deviations between density data obtained by integration and REFPROP[10] data. As it can be seen, our results are in good agreement with the available densities as long as they fall within ± 0.1 %. The (p,

Table 6. Calculated Densities, ρ, for Liquid (51 wt % R143a + 49 wt % R125) as a Function of Temperature T and Pressure p

p	ρ/(kg·m^{-3})							
MPa	T = 260 K	T = 270 K	T = 280 K	T = 290 K	T = 295 K	T = 300 K	T = 310 K	T = 320 K
1.0	1205.7	1168.7	1128.5					
3.0	1215.1	1179.9	1142.3	1101.4	1079.4	1056.2	1004.5	942.0
5.0	1223.8	1190.2	1154.6	1116.6	1096.4	1075.3	1030.0	978.7
10.0	1243.4	1212.7	1180.9	1147.7	1130.5	1112.8	1075.9	1036.8
15.0	1260.5	1231.9	1202.7	1172.7	1157.4	1141.7	1109.4	1076.0
20.0	1275.9	1248.9	1221.6	1193.9	1179.8	1165.6	1136.4	1106.5
25.0	1289.8	1264.1	1238.4	1212.4	1199.3	1186.0	1159.2	1131.8
30.0	1302.6	1278.0	1253.4	1228.9	1216.5	1204.1	1178.9	1153.4
35.0	1314.5	1290.8	1267.2	1243.8	1232.1	1220.3	1196.5	1172.5
40.0	1325.7	1302.7	1279.9	1257.4	1246.2	1235.0	1212.4	1189.6
45.0	1336.1	1313.8	1291.8	1270.1	1259.3	1248.5	1226.9	1205.1
50.0	1346.0	1324.3	1302.9	1281.8	1271.4	1261.1	1240.3	1219.4
55.0	1355.3	1334.2	1313.3	1292.9	1282.8	1272.8	1252.7	1232.6
60.0	1364.2	1343.6	1323.2	1303.3	1293.5	1283.8	1264.4	1245.0
65.0	1372.7	1352.5	1332.6	1313.1	1303.6	1294.1	1275.3	1256.5

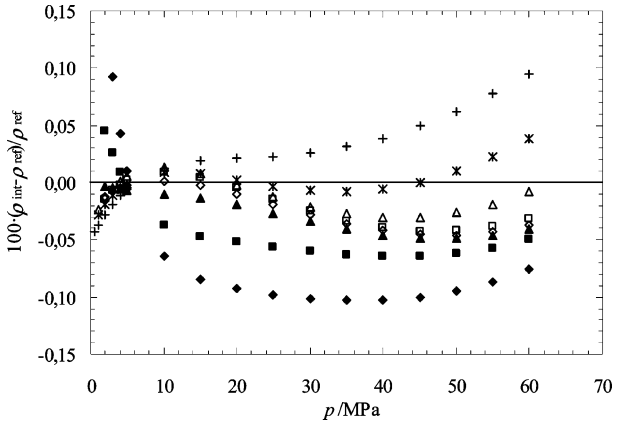

Figure 4. Plot of deviations between the density calculated by integration, ρ_{int}, from REFPROP[10] density data, ρ_{ref}: +, 260 K; ∗, 270 K; △, 280 K; □, 290 K; ◇, 295 K; ▲, 300 K; ■, 310 K; ◆, 320 K.

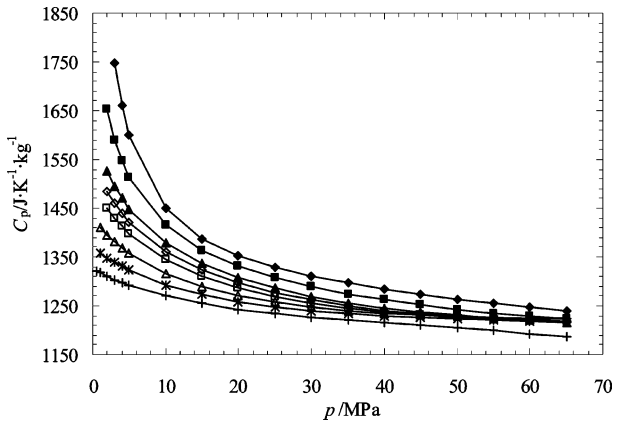

Figure 5. Isobaric heat capacity, C_p, of liquid (51 wt % R143a + 49 wt % R125), calculated through the integration procedure: +, 260 K; ∗, 270 K; △, 280 K; □, 290 K; ◇, 295 K; ▲, 300 K; ■, 310 K; ◆, 320 K.

C_p, T) data points are plotted in Figure 5 and Table 7. The deviation of the calculated isobaric heat capacities to REFPROP[10] estimates is smaller than 1.6 %. The other thermodynamic properties calculated are represented in Figures 6 to 8 and in Tables 8 to 10.

As far as we are aware, most of the available literature data were measured for different compositions. In some cases, the true R507 mixture was evaluated, but even here, there is a composition difference to our mixture. However, these data were used in REFPROP[10] to refine the EOS for the mixture. Consequently, the program fits the experimental data available.

Critical Behavior. Our acoustic method was applied to investigate the critical properties of the system xCO$_2$ + (1 − x)(51 wt % R143a + 49 wt % R125) covering all the composition range. The refrigerant used in this study is a near azeotropic mixture, which means that its behavior is similar to that one of a pure component. We have considered the mixture (51 wt % R143a + 49 wt % R125) as a pure component and treated the mixture with CO$_2$ as a binary mixture and not a ternary one. The estimated errors of the critical parameters reported are ± 0.1 K for the critical temperature and 0.05 MPa for the critical pressure. The estimate was based on a comparison of the results of different experiments performed with the same mixture and is mainly determined by the narrowness of the isotherms studied during an experiment as the pressure decreases in a continuous way.

(51 wt % R143a + 49 wt % R125). The acoustic experiments are carried out at constant temperature, and the pressure is lowered until a maximum in time delay is observed, meaning that it has reached a local maximum in the compressibility, corresponding to a phase transition. The temperature and pressure values corresponding to the absolute maximum of time delay in the ensemble of the isothermal curves is taken as the critical temperature and pressure of the fluid mixture under study. The critical parameters of the (51 wt % R143a + 49 wt % R125) mixture determined by our acoustic measurements were 344.04 K for critical temperature and 3.71 MPa for critical pressure.

Higashi[27] measured the critical parameters of the R143a + R125 mixture for different compositions. To represent the composition dependence of the critical parameters of the system, the author formulated a correlation of the critical locus, having his correlation given at 343.82 K for the critical locus of (51 wt % R143a + 49 wt % R125). Other authors measured the critical point of the mixture (50 wt % R143a + 50 wt % R125) by observation of the vanishing meniscus between the liquid and vapor phases.[26,28] Fröba et al.[26] reported a critical temperature for R507 (50 wt % R143a + 50 wt % R125), the refrigerant mixture commercially available from Solvay, of 344.06 K. Kishizawa et al.[28] and Higashi[27] determined slightly lower critical temperatures for the same mixture of (343.783 and 343.76) K, respectively. These data deviate less than 0.1 % in temperature from the gas−liquid critical values obtained by our acoustic method. Differences in sample purity and other experimental factors might explain these deviations. However, it can be concluded that the acoustic results are in good agreement with reported literature values.

CO$_2$ + (51 wt % R143a + 49 wt % R125). The critical line of CO$_2$ + (51 wt % R143a + 49 wt % R125) mixture was

Table 7. Calculated Isobaric Heat Capacity, C_p, for Liquid (51 wt % R143a + 49 wt % R125) as a Function of Temperature T and Pressure p

p	C_p/(J·kg^{-1}·K^{-1})							
MPa	T = 260 K	T = 270 K	T = 280 K	T = 290 K	T = 295 K	T = 300 K	T = 310 K	T = 320 K
1.0	1318	1359	1410					
3.0	1304	1339	1380	1430	1460	1495	1590	1749
5.0	1292	1323	1357	1398	1422	1449	1512	1599
10.0	1270	1293	1317	1345	1361	1378	1415	1450
15.0	1255	1273	1290	1311	1323	1336	1364	1388
20.0	1243	1259	1272	1287	1296	1307	1332	1352
25.0	1234	1248	1258	1269	1277	1286	1308	1329
30.0	1227	1241	1248	1256	1262	1270	1290	1311
35.0	1221	1235	1240	1246	1250	1257	1275	1296
40.0	1215	1230	1235	1238	1241	1246	1262	1284
45.0	1209	1227	1231	1232	1233	1237	1252	1273
50.0	1204	1224	1228	1227	1228	1230	1243	1264
55.0	1199	1221	1226	1224	1223	1225	1235	1255
60.0	1193	1219	1224	1221	1220	1220	1228	1247
65.0	1187	1217	1224	1220	1217	1217	1222	1240

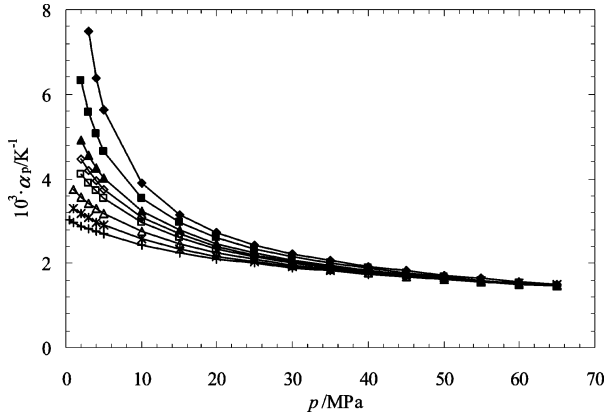

Figure 6. Thermal expansion coefficient, α_p, of liquid (51 wt % R143a + 49 wt % R125), calculated through the integration procedure: +, 260 K; ∗, 270 K; △, 280 K; □, 290 K; ◇, 295 K; ▲, 300 K; ■, 310 K; ◆, 320 K.

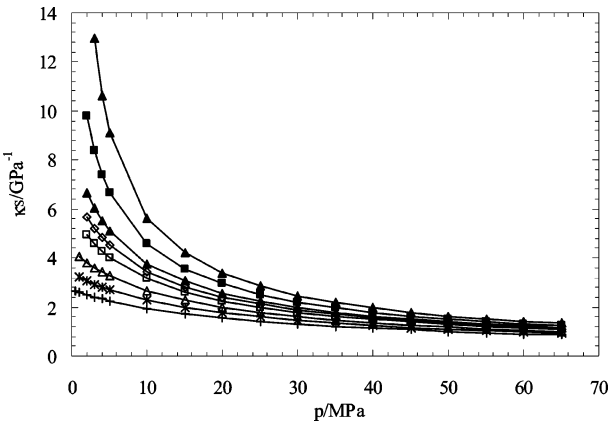

Figure 7. Isentropic compressibility, κ_S, of liquid (51 wt % R143a + 49 wt % R125), calculated through the integration procedure: +, 260 K; ∗, 270 K; △, 280 K; □, 290 K; ◇, 295 K; ▲, 300 K; ■, 310 K; ◆, 320 K.

determined over the whole composition range. Acoustic measurements were performed on seven mixtures. The experimental critical parameters, T_c and p_c, are shown in Table 11 for each mixture and are plotted in Figure 9. The system exhibits type I fluid phase behavior, according to the classification of van Konynenburg and Scott,[29] which means that a continuous critical line connects the critical points of (51 wt % R143a + 49 wt % R125) and CO_2. This system behaves almost ideally. (51 wt % R143a + 49 wt % R125), as we concluded in previous studies

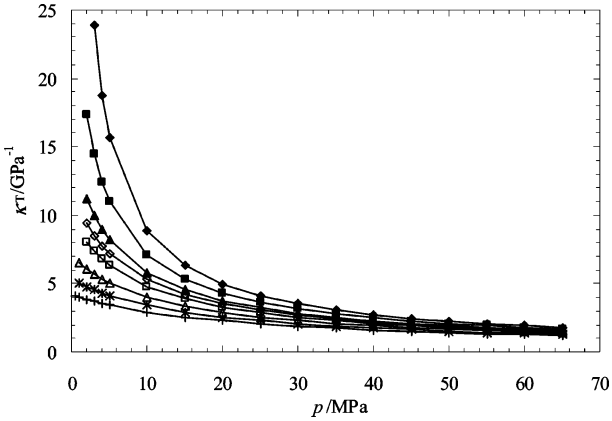

Figure 8. Isothermal compressibility, κ_T, of liquid (51 wt % R143a + 49 wt % R125) calculated through the integration procedure: +, 260 K; ∗, 270 K; △, 280 K; □, 290 K; ◇, 295 K; ▲, 300 K; ■, 310 K; ◆, 320 K.

for R404A and R410A, should be also a useful modifier for CO_2. Its relatively low critical temperature (344.04 K) and its miscibility with CO_2 make it potentially attractive as modifier for improving solubility in supercritical CO_2. As can be seen from Figure 9, the critical pressure of the system goes from p_c of pure CO_2 down to 3.72 MPa, the critical pressure of (51 wt % R143a + 49 wt % R125). This means that as (51 wt % R143a + 49 wt % R125) is added to CO_2, the solvation properties of the mixture will have substantially changed but the critical temperature and critical pressure remain reasonably low.

Correlation of Results and Discussion. Experimental critical data were correlated with the Peng−Robinson equation of state (PR EOS)[30] that is a cubic EOS based on a one-fluid model:

$$p = \frac{RT}{(V_m - b)} - \frac{a(T)}{V_m(V_m + b) + b(V_m - b)} \qquad (11)$$

using the van der Waals one-fluid mixing rules, which assume random distribution of molecules:

$$a = x_1^2 a_1 + 2x_1 x_2 a_{12} + x_2^2 a_2 \qquad (12)$$

$$b = x_1^2 b_1 + 2x_1 x_2 b_{12} + x_2^2 b_2 \qquad (13)$$

In these equations x_i is the mole fraction of component i (i = 1, 2), and a_i and b_i are pure component parameters defined by Peng and Robinson.[30] In particular, $a_i(T) = a_{c,i}(T_{c,i})\ \alpha_i(T, \beta_i(\omega_i))$, where ω_i is Pitzer's acentric factor of molecule i. The

Table 8. Calculated Isobaric Thermal Expansion Coefficient, α_p, for Liquid (51 wt % R143a + 49 wt % R125) as a Function of Temperature *T* and Pressure *p*

p	$10^3\alpha_p/K^{-1}$							
MPa	*T* = 260 K	*T* = 270 K	*T* = 280 K	*T* = 290 K	*T* = 295 K	*T* = 300 K	*T* = 310 K	*T* = 320 K
1.0	2.971	3.287	3.738					
3.0	2.823	3.072	3.422	3.893	4.188	4.543	5.575	7.485
5.0	2.692	2.898	3.177	3.540	3.759	4.009	4.653	5.646
10.0	2.441	2.572	2.745	2.963	3.088	3.224	3.528	3.895
15.0	2.256	2.342	2.455	2.601	2.683	2.772	2.959	3.156
20.0	2.111	2.169	2.245	2.346	2.405	2.467	2.599	2.725
25.0	1.994	2.034	2.084	2.155	2.198	2.244	2.343	2.436
30.0	1.897	1.924	1.956	2.005	2.037	2.072	2.150	2.224
35.0	1.813	1.833	1.851	1.884	1.907	1.935	1.998	2.059
40.0	1.741	1.755	1.764	1.784	1.801	1.822	1.873	1.926
45.0	1.676	1.689	1.690	1.700	1.711	1.726	1.768	1.815
50.0	1.619	1.630	1.627	1.628	1.634	1.645	1.678	1.720
55.0	1.566	1.578	1.571	1.565	1.568	1.575	1.601	1.637
60.0	1.517	1.532	1.521	1.511	1.510	1.513	1.532	1.564
65.0	1.471	1.489	1.477	1.462	1.458	1.458	1.471	1.499

Table 9. Calculated Isentropic Compressibility, κ_S, for Liquid (51 wt % R143a + 49 wt % R125) as a Function of Temperature *T* and Pressure *p*

p	κ_S/GPa^{-1}							
MPa	*T* = 260 K	*T* = 270 K	*T* = 280 K	*T* = 290 K	*T* = 295 K	*T* = 300 K	*T* = 310 K	*T* = 320 K
1.0	2.598	3.202	4.057					
3.0	2.412	2.921	3.609	4.578	5.224	6.027	8.399	12.977
5.0	2.254	2.692	3.263	4.029	4.516	5.096	6.656	9.110
10.0	1.948	2.268	2.662	3.152	3.443	3.772	4.570	5.618
15.0	1.726	1.975	2.270	2.621	2.823	3.045	3.560	4.193
20.0	1.555	1.757	1.990	2.259	2.410	2.574	2.943	3.379
25.0	1.419	1.588	1.778	1.993	2.112	2.239	2.520	2.844
30.0	1.308	1.451	1.611	1.789	1.885	1.988	2.211	2.463
35.0	1.215	1.339	1.475	1.626	1.706	1.791	1.975	2.178
40.0	1.136	1.244	1.363	1.492	1.561	1.633	1.788	1.956
45.0	1.067	1.164	1.268	1.381	1.441	1.504	1.636	1.780
50.0	1.007	1.093	1.187	1.287	1.340	1.395	1.511	1.635
55.0	0.954	1.032	1.116	1.207	1.254	1.303	1.406	1.515
60.0	0.906	0.978	1.055	1.137	1.180	1.224	1.317	1.414
65.0	0.863	0.929	1.000	1.076	1.115	1.155	1.240	1.328

Table 10. Calculated Isothermal Compressibility, κ_T, for Liquid (51 wt % R143a + 49 wt % R125) as a Function of Temperature *T* and Pressure *p*

p	κ_T/GPa^{-1}							
MPa	*T* = 260 K	*T* = 270 K	*T* = 280 K	*T* = 290 K	*T* = 295 K	*T* = 300 K	*T* = 310 K	*T* = 320 K
1.0	4.043	5.038	6.517					
3.0	3.720	4.533	5.688	7.368	8.506	9.948	14.430	23.860
5.0	3.445	4.132	5.066	6.357	7.189	8.192	10.964	15.628
10.0	2.929	3.407	4.018	4.801	5.272	5.805	7.106	8.849
15.0	2.562	2.919	3.357	3.897	4.211	4.556	5.354	6.328
20.0	2.286	2.565	2.898	3.298	3.525	3.772	4.326	4.967
25.0	2.069	2.295	2.558	2.868	3.042	3.230	3.643	4.106
30.0	1.894	2.082	2.296	2.544	2.682	2.830	3.154	3.509
35.0	1.748	1.908	2.086	2.290	2.403	2.524	2.786	3.070
40.0	1.625	1.764	1.915	2.086	2.180	2.280	2.498	2.733
45.0	1.519	1.641	1.771	1.917	1.997	2.083	2.267	2.466
50.0	1.427	1.536	1.650	1.776	1.845	1.919	2.078	2.250
55.0	1.346	1.445	1.546	1.656	1.716	1.780	1.919	2.070
60.0	1.274	1.364	1.455	1.553	1.606	1.662	1.785	1.919
65.0	1.209	1.293	1.375	1.463	1.510	1.560	1.670	1.790

combining rules for the binary cross-interaction parameters a_{12} and b_{12} are given by

$$a_{12} = (a_1 a_2)^{1/2}(1 - k_{12}) \tag{14}$$

$$b_{12} = \frac{1}{2}(b_1 + b_2)(1 - l_{12}) \tag{15}$$

Here, k_{12} and l_{12} are parameters describing deviations from, respectively, the geometric and arithmetic mean combining rules. Values of critical temperature, critical pressure, and acentric factor[31,32] for each pure fluid, which are presented in Table 12,

Table 11. Experimental Critical Data, p_c and T_c, of the System CO_2 + (51 wt % R143a + 49 wt % R125)

x_{CO_2}	p_c/MPa	T_c/K	x_{CO_2}	p_c/MPa	T_c/K
0.974	7.30	305.50	0.780	6.55	315.80
0.940	7.15	306.82	0.290	4.65	335.59
0.900	6.99	308.79	0.000	3.71	344.04

constitute along with the deviation parameters the model input variables for PR EOS. The acentric factor of (51 wt % R143a + 49 wt % R125) was calculated using the definition of Pitzer[33] and the experimental data T_c, p_c, and vapor pressures reported by Solvay Technical Data Sheets.[2] The deviation parameters, k_{12} and l_{12}, were varied so that the theoretical critical line would

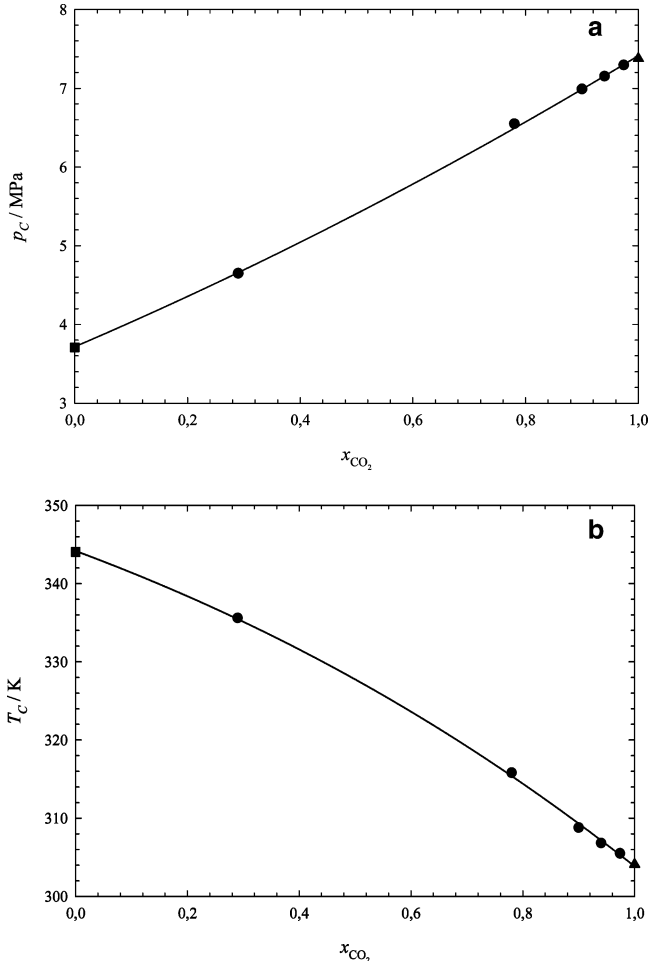

Figure 9. Projections of the critical curve for the $x\mathrm{CO_2} + (1 - x)$(51 wt % R143a + 49 wt % R125) system: (a) $p-x$ projection; (b) $T-x$ projection.

Table 12. Parameters of the Pure Substances Used in the Peng−Robinson Equation of State

component	p_c/MPa	T_c/K	ω_i
CO_2	7.38[34,35]	304.13[35]	0.239[36]
R507	3.7[22]	343.95	0.288

give the best fit of the experimental data for each binary system. Although the deviation parameters are often fitted to the experimental critical data using only the equimolar mixture,[19] we have used all the experimental data available for evaluating these parameters. The deviation parameters of CO_2 + (51 wt % R143a + 49 wt % R125) that gave the best fit were $k_{12} = 0.00017$ and $l_{12} = 0.01$. Figure 10 shows the (p, T) projection of the critical line for this system using the optimized interaction parameters and the pure component vapor pressures for the binary system. It is also depicted for comparison the (p, T) projections of the critical line of CO_2 + R404A[4] and CO_2 + R410A.[5] It can be seen from this figure that the critical behavior of both systems CO_2 + R404A and CO_2 + (51 wt % R143a + 49 wt % R125) is almost coincidental, meaning that the addition of 4 wt % of 1,1,1,2-tetrafluoroethane (R134a) did not significantly change the critical properties of the overall mixture.

Conclusions

The thermophysical properties and critical parameters for the alternative refrigerant mixture (51 wt % of 1,1,1-trifluoroethane (R143a) + 49 wt % of pentafluoroethane (R125)) were investigated using two different acoustic techniques. Several derived thermodynamic and thermophysical data along a broad

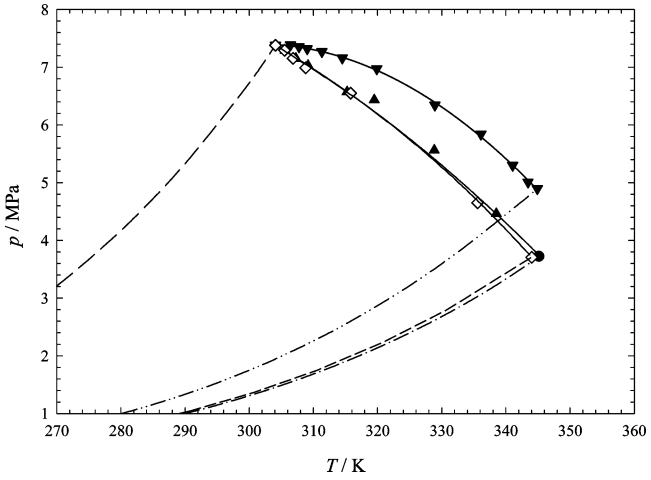

Figure 10. Comparison of $p-T$ projections of the critical lines of mixtures of CO_2 with different refrigerants, covering all composition ranges: ▲, acoustic data for $x\mathrm{CO_2} + (1 - x)$(51 wt % R143a + 49 wt % R125) system; ●, acoustic data for $x\mathrm{CO_2} + (1 - x)$R404A system; ◇, acoustic data for $x\mathrm{CO_2} + (1 - x)$R410A system; —, predicted critical lines with PR-EOS for each system; − −, vapor pressure curve for CO_2;[36] − · −, vapor pressure curve for (51 wt % R143a + 49 wt % R125);[2] − · · −, vapor pressure curve for R410A[2]; - - -, vapor pressure curve for R404A.[2]

(p, T) range were calculated with less error than experimental measurements, which were difficult to implement. The critical behavior of the system $x\mathrm{CO_2} + (1 - x)$(51 wt % R143a + 49 wt % R125) was also investigated over the whole composition range. With mole fractions of up to 10 % of (51 wt % R143a + 49 wt % R125), critical temperature only increases 4.7 K and the critical pressure decreases 0.31 MPa. The critical line shows type I fluid phase behavior. The results were well-correlated with the PR EOS using conventional mixing and combining rules.

Literature Cited

(1) Li, J.; Tillner-Roth, R.; Sato, H.; Watanabe, K. Equation of state for hydrofluorocarbon refrigerant mixtures of HFC125/143a, HFC125/134a, HFC134a/143a and HFC125/134a/143a. *Fluid Phase Equilib.* **1999**, *161*, 225−229.

(2) Solkane 507 Solvay Fluor und Derivate Leaflet. Technical Data Sheets; http://www.solvay.com.

(3) Jannick, P.; Meurer C. Replacement of R22 and future trends in refrigeration and in air conditioning. *Solvay Fluor und Derivate GmbH 10th International Conference*, Jaszbereny, Hungary, 2000; 30.8−1.9, pp 1, 9.

(4) Esperança, J. M. S. S.; Pires, P. F.; Guedes, H. J. R.; Ribeiro, N.; Costa, T.; Aguiar-Ricardo, A. Acoustic determination of thermophysical properties and critical parameters of R404A and critical line of $x\mathrm{CO_2} + (1 - x)$R404A. *J. Chem. Eng. Data* **2006**, *51*, 1148−1155.

(5) Ribeiro, N.; Costa, T.; Aguiar-Ricardo, A.; Esperança, J. M. S. S.; Pires, P. F.; Guedes, H. J. R. Acoustic determination of thermophysical properties and critical parameters of R410A and critical line of $x\mathrm{CO_2} + (1 - x)$R410A *J. Chem. Eng. Data* **2006**, *51*, 1906−1914.

(6) Pires, P. F.; Guedes, H. J. R. The speed of sound and isentropic compressibility of liquid difluoromethane (HFC32) from $T =$ (248 to 343) K and pressures up to 65 MPa. *J. Chem. Thermodyn.* **1999**, *31*, 55−69.

(7) Pires, P. F.; Guedes, H. J. R. The speed of sound and derived thermodynamic properties of liquid trifluoromethane (HFC23) from $T =$ (258 to 303) K and pressures up to 65 MPa. *J. Chem. Thermodyn.* **1999**, *31*, 479−490.

(8) Pires, P. F.; Esperança, J. M. S. S.; Guedes, H. J. R. Ultrasonic speed of sound and derived thermodynamic properties of liquid 1,1,1,2,3,3,3-heptafluoropropane (HFC227ea) from 248 K to 333 K and pressures up to 65 MPa. *J. Chem. Eng. Data* **2000**, *45*, 496−501.

(9) Gomes de Azevedo, R.; Szydlowski, J.; Pires, P. F.; Esperança, J. M. S. S.; Guedes, H. J. R.; Rebelo, L. P. N. A novel non-intrusive microcell for sound-speed measurements in liquids. Speed of sound and thermodynamic properties of 2-propanone at pressures up to 160 MPa. *J. Chem. Thermodyn.* **2004**, *36*, 211−222.

(10) McLinden, M. O.; Klein, S. A.; Lemmon, E. W.; Peskin, A. P. *REFPROP*, NIST Standard Reference Database 23. Version 6.01; Standard Reference Data Program: Gaithersburg, MD, 1998.
(11) Muringer, M. J. P.; Trappeniers, N. J.; Biswas, S. N. The effect of pressure on the sound-velocity and density of toluene and *n*-heptane up to 2600 bar. *Phys. Chem. Liq.* **1985**, *14*, 273−296.
(12) Daridon, J. L.; Lagrabette, A.; Lagourette, B. Speed of sound, density, and compressibilities of heavy synthetic cuts from ultrasonic measurements under pressure. *J. Chem. Thermodyn.* **1998**, *30*, 607−623.
(13) Sun, T.; Biswas, S. N.; Trappeniers, N. J. Seldam; C. A. T. Acoustic and thermodynamic properties of methanol from 273 to 333 K and at pressures up to 280 MPa. *J. Chem. Eng. Data* **1988**, *33*, 395−398.
(14) Trusler, J. P. M. *Physical Acoustics and Metrology of Fluids*; Adam Hilger: Bristol, 1991.
(15) Kordikowski, A.; Robertson, D. G.; Aguiar-Ricardo, A.; Popov, V. K.; Howdle, S. M.; Poliakoff, M. Probing vapor/liquid equilibria of near-critical binary gas mixtures by acoustic measurements. *J. Phys. Chem.* **1996**, *100*, 9522−9526.
(16) Kordikowski, A.; Robertson, D. G.; Poliakoff, M.; DiNoia, T. D.; McHugh, M.; Aguiar-Ricardo, A. Acoustic determination of the critical surfaces in the ternary systems $CO_2 + CH_2F_2 + CF_3CH_2F$ and $CO_2 + C_2H_4 + CH_3CHCH_2$ and in their binary subsystems. *J. Phys. Chem. B* **1997**, *101*, 5853−5862.
(17) Ribeiro, N.; Casimiro, T.; Duarte, C.; Poliakoff, M.; Nunes da Ponte, M.; Aguiar-Ricardo, A. Vapor−liquid equilibrium and critical line of the $CO_2 + Xe$ system. Critical behavior of the $CO_2 + Xe$ versus CO_2 + *n*-alkanes. *J. Phys. Chem. B* **2000**, *104*, 791−795.
(18) Ribeiro, N.; Aguiar-Ricardo, A. A simple acoustic probe for fluid phase equilibria: application to the $CO_2 + N(C_2H_5)_3$ system. *Fluid Phase Equilib.* **2001**, *185*, 295−303.
(19) Ribeiro, N.; Aguiar-Ricardo, A.; Kordikowski, A.; Poliakoff, M. Acoustic determination of the critical surface of $\{x_1CO_2 + x_2C_2H_6 + (1 - x_1 - x_2CHF_3\}$. *Phys. Chem. Chem. Phys.* **2001**, *3*, 1027−1033.
(20) Aguiar-Ricardo, A.; Temtem, M.; Casimiro, T.; Ribeiro, N. A visual acoustic high-pressure cell for the study of critical behavior of non-simple mixtures. *Rev. Sci. Instrum.* **2004**, *75*, 3200−3202.
(21) Aguiar-Ricardo, A.; Casimiro, T.; Costa, T.; Leandro, J.; Ribeiro, N. Visual and acoustic investigation of the critical behavior of mixtures of CO_2 with a perfluorinated polyether. *Fluid Phase Equilib.* **2006**, *239*, 26−29.
(22) Reis, J. C. R.; Ribeiro, N.; Aguiar-Ricardo, A. Can the speed of sound be used for detecting critical states of fluid mixtures? *J. Phys. Chem. B* **2006**, *110*, 478−484.
(23) Kyohara, O.; Alpin, C. J.; Benson, G. C. Ultrasonic velocities, compressibilities, and heat capacities for binary mixtures of benzene, cyclohexane, and tetrachloromethane at 298.15 K. *J. Chem. Thermodyn.* **1978**, *10*, 721−730.
(24) Lainez, A.; Miller, J. F.; Zollweg, J. A.; Streett, W. B. Volumetric and speed-of-sound measurements for liquid tetrachloromethane under pressure. *J. Chem. Thermodyn.* **1987**, *19*, 1251−1260.
(25) Sun, T. F.; Kortbeek, P. J.; Trappeniers, N. J.; Biswas, S. N. Acoustic and thermodynamic properties of benzene and cyclohexane as a function of pressure and temperature. *Phys. Chem. Liq.* **1987**, *16*, 163−178.
(26) Fröba, A. P.; Will, S.; Leipertz, A. Thermophysical properties of binary and ternary fluid mixtures from dynamic light scattering. *Int. J. Thermophys.* **2001**, *22*, 1349−1368.
(27) Higashi, Y. Vapor−liquid equilibrium, coexistence curve, and critical locus for pentafluoroethane + 1,1,1-trifluoroethane (R125//R143a). *J. Chem. Eng. Data* **1999**, *44*, 333−337.
(28) Kishizawa, G.; Sato, H.; Watanabe, K. Measurements of saturation densities in critical region and critical loci for binary R-32/125 and R-125/143a systems. *Int. J. Thermophys.* **1999**, *20*, 923−932.
(29) van Konynenburg, P. H.; Scott, R. L. *Philos. Trans. R. Soc. London, A* **1980**, *298*, 495.
(30) Peng, D.; Robinson, D. New two-constant equation of state. *Ind. Eng. Chem. Fundam.* **1976**, *15*, 59−64.
(31) Sandler, S. I.; Orbey, H.; Lee, B.-I. In *Models for Thermodynamic and Phase Equilibria Calculations*; Sandler, S. I., Ed.; Marcel Dekker: New York, 1994; p 87.
(32) Prausnitz, J. M.; Lichtenthaler, R. N.; De Azevedo, E. G. *Molecular Theory of Fluid-Phase Equilibria*, 3rd ed.; Prentice Hall: Upper Saddle River, NJ, 1999; p 718.
(33) Pitzer, K. S. The volumetric and thermodynamic properties of fluids. I. Theoretical basis and virial coefficients. *J. Am. Chem. Soc.* **1955**, *77*, 3427−3433.
(34) Angus, S.; Armstrong, B. B.; de Reuck, K. M. *Carbon Dioxide−International Thermodynamic Tables of the Fluid State-3*; IUPAC/Pergamon Press: Oxford, U.K., 1976.
(35) Span, R.; Wagner, W. A new equation of state for carbon dioxide covering the fluid region from the triple-point temperature to 1100 K at pressures up to 800 MPa. *J. Phys. Chem. Ref. Data* **1996**, *25*, 1509−1596.
(36) Reid, R. C.; Prausnitz, J. M.; Pauling, B. E. *The Properties of Gases and Liquids*, 4th ed.; McGraw-Hill: New York, 1987.

Received for review June 26, 2006. Accepted August 23, 2006. Financial support from Fundação para a Ciência e Tecnologia (FCT), FEDER, and FSE through Contracts PBIC/C/QUI/2134/95, POCTI/QUI/35429/2000, PraxisXXI/BD/16081/98, Praxis XXI/BD/19836/99, and Fundação Calouste Gulbenkian are gratefully acknowledged.

JE060291C